INVESTIGATION OF OXYGEN REDUCTION MECHANISMS USING CATHODE MICROELECTRODES, PART II: ANALYTICAL MODELLING OF $La_{(1-x)}Sr_xMnO_{3-d}$ ELECTROCHEMICAL IMPEDANCE SPECTRUM

Bilge Yildiz[a], Gerardo Jose la O'[b], Yang Shao-Horn[b]
[a]Argonne National Laboratory, Argonne, IL 60439, USA
[b]Electrochemical Energy Laboratory, Massachusetts Institute of Technology, Cambridge, MA 02139, USA

ABSTRACT

The oxygen reduction reactions (ORR) on $La_{1-x}Sr_xMnO_{3-d}$ (LSM) are not well understood at the molecular level. We couple the kinetic modeling of the oxygen reduction process with experiments on patterned microelectrode cathodes for analyzing the electrochemical impedance spectroscopy (EIS) response to investigate ORR. This paper presents the analytical modeling of EIS response due to specified oxygen reduction mechanisms on LSM. A model for ORR as proposed in literature with surface adsorption, electronation, diffusion and electrolyte diffusion is considered as a likely realistic reaction mechanism and is examined here. The intrinsic electrochemical properties for LSM are partially retrieved from literature. The EIS response of this model implies that the electrode surface processes can govern the high frequency region and the electrode surface and electrolyte bulk diffusion can govern the low frequency region in the EIS. A comparison of the simulated and experimental EIS as a function of P_{O2} indicates discrepancy between the two. The ORR model requires modifications and alternatives are proposed for further investigation.

INTRODUCTION

The power of a solid oxide fuel cell (SOFC) is limited by the current associated with oxygen reduction at the cathode under a given operating voltage. Although oxygen reduction at SOFC cathodes has been studied in the literature, a comprehensive and clear description of the reaction mechanisms has not been discovered. Electrochemical impedance spectroscopy (EIS) reveals the distribution of relaxation times and the amplitude of system impedance over a range of frequencies. The theory of impedance spectroscopy specifically for solid systems can be found in Ref. 1. Any intrinsic property that influences the conductivity of an electrode/electrolyte system, or an external stimulus can be studied by (EIS). Therefore, experimental EIS measurements have been widely used in studying the oxygen reduction mechanism on the $La_{1-x}Sr_xMnO_{3-d}$ (LSM) cathodes linked to a yttria-stabilized zirconium (YSZ) electrolyte (2-7). The resonant frequency and activation energy for a specific process, which should be configuration and materials specific, are also reported in Refs. 2-7. Nevertheless, significant discrepancies and ambiguities are observed for in resonant frequencies and activation energies of elementary oxygen reduction reaction steps. This discrepancy indicates to a lack of fundamental understanding of oxygen reduction process(es) at the LSM/YSZ interface at the molecular level.

Electrical equivalent circuits have usually been fit to the impedance data for representing the characteristic resistances and capacitances in the SOFC behavior. All implications presented in Refs. 2-7 have been based on equivalent circuit fitting to the EIS measurements. This approach does not comprise a physical meaning to distinguish the mechanisms that constitute the oxygen reduction process. Therefore, it can mislead the interpretation of impedance spectroscopy and limit the comprehension of the kinetics of physical processes.

A kinetic model that captures the physical aspects of oxygen reduction can yield both the resistive and capacitive consequences from the individual processes in oxygen reduction. Thus, a dynamic model of the ORR scheme on the LSM/YSZ is required to simulate its AC impedance response and guide the interpretation of experimental EIS measurements. A similar kinetic modeling approach has been implemented in Refs. 8-11. In this work, we first develop representative physical models for LSM/YSZ reactions and reconcile simulated results with experimental and previously reported AC impedance data on LSM/YSZ system in order to reveal the details of the oxygen reduction mechanism at molecular level.

NON-LINEAR ELECTROCHEMICAL KINETIC MODELING

Experiments and information from literature can be used for promoting an electrochemical model for the oxygen reduction reaction steps and a range for their kinetic parameters. An equivalent mathematical model can be developed based upon the electrochemical model, and be simulated with different operating conditions for validating the proposed electrochemical model and for verifying the appropriate kinetic parameters. If necessary, a combination of electrochemical models can be tested in this manner.

A Mathematical Model for Representing the AC Impedance Response from SOFC Cathodic Reaction Mechanism

Figure 1 represents the modeling framework in this work for finding a consistent of reaction schemes and kinetic parameters to describe the oxygen reduction mechanism for the LSM/YSZ system. The approach here is not specific for a certain materials system, but can in principle be adapted to any electrochemical interface.

Independent of the exact form of the intermediate reaction steps, the time dependence of the intermediate species concentrations in oxygen reduction can be expressed as:

$$\underline{X} = \frac{\partial \underline{C}}{\partial t} = \underline{x}(\underline{C}, \underline{k}, \eta(t)) \qquad [1]$$

where, for a given temperature, P_{O2} and set of material properties, $\underline{C}$ is the array of concentrations for the intermediate species, $\underline{k}$ is the array of kinetic parameters (such as forward and backward reaction rate constants for each step, diffusion constants and activation energies), and $\eta(t)$ is the time-dependent overpotential (input parameter) applied on the cell. Consequently, the Faradaic current (output function) can be expressed in terms of the net rate of the electron transfer step, which reflects the AC impedance response as:

$$Q = I_F = q(C, k, \eta(t)) = -n_e FA(k_n C_n - k_{-n} C_{-n}) \qquad [2]$$

where n represents the electron transfer steps, and C_n and C_{-n} are the concentration of the unreduced and reduced oxygen, respectively, independent of the location in the system. The exact form of the Eqs 1 and 2 depends on the proposed consecutive reaction steps that

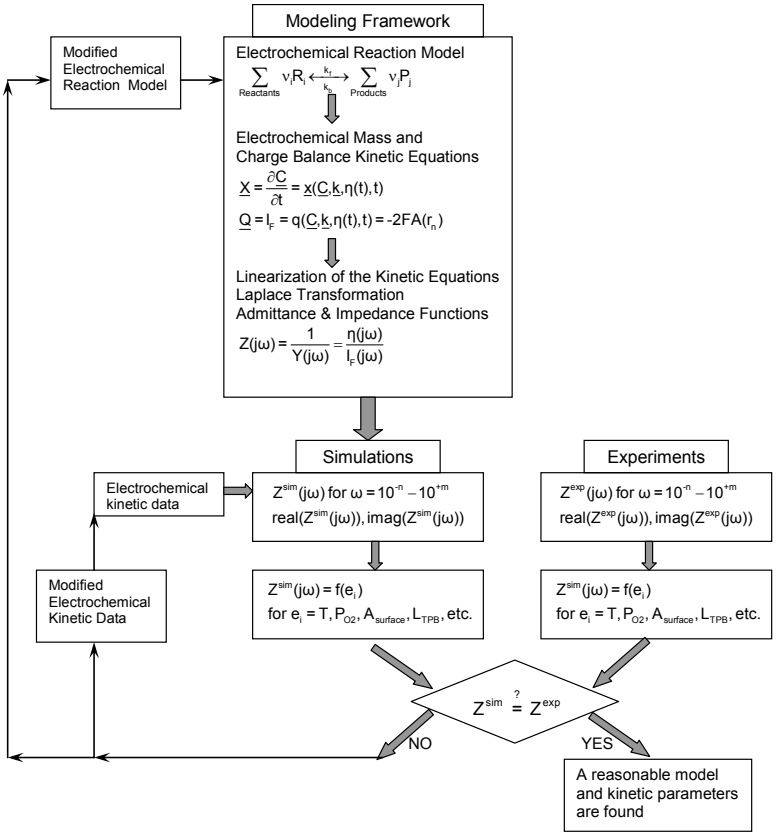

Figure 1: Electrochemical kinetic modeling approach for the identification of reaction mechanism at SOFC cathode.

constitute the electrode reactions. The time-dependent reaction rates based on charge and mass balance can include as many steps as necessary without having to assume any particular step as rate determining. In determining the kinetic behavior of intermediate species concentrations and the output current, it is important to realize that the resulting output current depends on each of the intermediate reaction species. However, the relative effect of each species' time-dependent concentration on the total current can be different.

The set of coupled differential equations that describe the time dependence of intermediate species and the intrinsic current (Eqs 1 and 2) can be solved by integration methods. This approach yields a numerical solution in time domain for the output current and can be converted to the frequency domain by Fourier or Laplace transforms for finding the resulting EIS response. Still, it is important to understand the physical meaning of the characteristics of the AC impedance spectrum. Our objective is to refer to the AC impedance response analytically for being able to associate certain physical mechanisms with characteristics of EIS response. Hence, we choose to find the characteristics of AC impedance response analytically in frequency domain by using an approach from control theory; *transfer function from state space representation* of a non-linear system. In our problem domain, the nonlinear electrochemical system described by the Equations 1 and 2 are well suited to the state space representation of a non-linear system. Many text books on control theory can give the details of this approach. This approach has been used recently in studying the electrode kinetics of Pt,O_2/YSZ and Ni, H_2/YSZ electrodes (8-11). However, the method was implemented as a numerical tool to fit/find/verify the reaction rate

constants for the presumed electrochemical model. Consequently, the results could not conclusively verify all the proposed electrochemical models because of yet limited accompanying experiments.

We implement the scheme summarized in Figure 1 for finding the AC impedance response. The mathematical modeling and simulations for obtaining the EIS of various electrochemical models are implemented by preparing programs in MATLAB®.

ELECTROCHEMICAL KINETICS MODEL FOR LSM/YSZ SYSTEM

The elementary reaction schemes that take place at the LSM cathode are the basis for the model simulations and for understanding the oxygen reduction kinetics. The overall oxygen reduction reaction can be represented as $O_{2(g)} + 4e^- + 2V_{\ddot{O}}^{Y} \Leftrightarrow 2O_0^Y$ [3] where $V_{\ddot{O}}^{Y}$ and O_0^Y refer to vacancies and oxygen ions in the YSZ electrolyte lattice, respectively. This reaction consists of multiple consecutive steps. Surface dominated schemes proposed for ORR on LSM are first considered in this work. Two of the proposed ORR models are presented in Table I. In order to identify key parameters controlling impedance characteristics and to test the robustness of the model described in this work, we perform the modeling from the most simple to the more complex reaction schemes. Analytical derivation and interpretation of the Model 1 is presented in the next section. Qualitative implications from and simulation of the more realistic but more complicated Model 2 is analyzed and presented subsequently.

Table I: Selected Reaction Models for Oxygen Reduction on LSM

STEPS	EQUATION	PROCESS / LOCATION	REACTION PARAMETERS
Model 1			
1	$O_{2(g)} \Leftrightarrow 2O_{ad,3PB}$	Dissociative adsorption on LSM 3-phase boundary (3PB)	-Adsorption / desorption reaction rate constants at 3PB; k_{ads}, k_{des} (k_1, k_{-1}) -Surface coverage of oxygen at 3PB; θ -Oxygen surface concentration; N_o
2	$O_{ad,3PB} + 2e^- + V_{\ddot{O}}^{Y} \Leftrightarrow O_O^Y$	Reduction of adsorbed oxygen and its transfer at 3PB into YSZ lattice	-Oxygen electronation and $O^=$ transfer rate constants at 3PB; k_2, k_{-2} -Surface coverage of oxygen at 3PB; θ
Model 2			
1	$O_{2(g)} \Leftrightarrow 2O_{ad,s}$	Dissociative adsorption along LSM surface	-Adsorption / desorption reaction rate constants on LSM surface; k_{ads}, k_{des} (k_1, k_{-1}) -Surface coverage of oxygen on LSM; θ -Oxygen surface concentration; N_o
2	$O_{ad,s} + 2e^- \Leftrightarrow O_s^{-2}$	Reduction of adsorbed oxygen along LSM surface	-Oxygen electronation rate constants; k_2, k_{-2} -Surface coverage of oxygen on LSM; θ -Fraction of reduced oxygen on LSM; α
3	$O_s^{-2} \Leftrightarrow O_{3PB}^{-2}$	Diffusion of oxygen in the electrolyte, in parallel to Steps 1 and 2	-Reduced oxygen diffusion coefficient on LSM surface; $D_{surface}$
4	$O_{3PB}^{-2} + V_{\ddot{O}}^{Y} \Leftrightarrow O_O^Y$	Transfer of reduced oxygen at the 3PB into YSZ lattice	-$O^=$ transfer rate constants at LSM-surface/YSZ interface; k_3, k_{-3}
5	$O_O^Y \Leftrightarrow O_O^{Y'}$	Diffusion of oxygen in the electrolyte	-Oxygen diffusion coefficient in bulk YSZ; D_{YSZ}

Model 1 and its Analysis

Model 1 is the simplest possible electrochemical model for oxygen reduction at LSM cathode. It involves the dissociative adsorption of oxygen at 3PB as the first step, and its reduction and transfer into the electrolyte as the second step. The linearization of the normalized governing equations with respect to the small changes in surface coverage and applied potential yield the Laplace transform of the state space representation. Consequently, the impedance obtained for this process is reduced to:

$$Z_F(\omega) = \frac{1}{\frac{\partial Q}{\partial \eta}} \times \left(\frac{s - \frac{\partial X}{\partial \theta}}{s - \frac{\partial X}{\partial \theta} + \frac{1}{2FAN_o} \frac{\partial Q}{\partial \theta}} \right) \quad [4]$$

where $s = j\omega$

The expression for the impedance of the process defined by Model 1 depends on three physical terms: change in the rate of change of adsorbed oxygen concentration with respect to surface coverage, $\frac{\partial X}{\partial \theta}$ (a negative term), change in the current with respect to surface coverage, $\frac{\partial Q}{\partial q}$ (a negative term), and change in the current with respect to the overpotential, $\frac{\partial Q}{\partial \eta}$ (a positive term). The characteristic parameters of the resulting impedance from the first order process Model 1, such as the high and low frequency limits and the resonant frequency, ω_r, are derived analytically and presented in Figure 2 qualitatively.

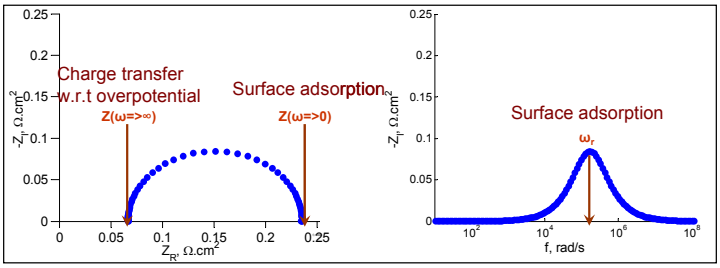

Figure 2: Governing physical mechanisms on EIS for ORR based on Model 1

A change in the value of reaction kinetic parameters, $\underline{k}$, influences each of the stated derivative terms in Eq 4 to affect the rate of charge transfer. A change in k_2 and k_{-2} determines the value of the high frequency limit of the impedance. It has little influence on the value of the semicircle diameter if the competition between $\frac{\partial Q}{\partial \theta}$ and $\frac{\partial Q}{\partial \eta}$ is nearly constant. A change in k_1 and k_{-1} chiefly controls the low frequency intercept of EIS and the ω_r.

Model 2 and its Analysis

As the complexity of the electrochemical model increases, the complexity of the analytically driven AC impedance increases significantly. Thus, we do not present the details of the derivation and interpretation of the results for more complex models here. A qualitative description of the findings for Model 2 is shown in Figure 3. If the simulated and experimental impedance data show the same tendencies with certain parametric variations, it can be concluded that the simulated electrochemical model might describe the kinetics of the system correctly. In doing so, to find the most relevant kinetic parameters for the model, it is reasonable to consider the entire system in a more realistic manner, although this can require more effort due to its complexity. In this study, Model 2 can be a more likely configuration of oxygen reduction reactions at LSM/YSZ system. Therefore, a quantita-

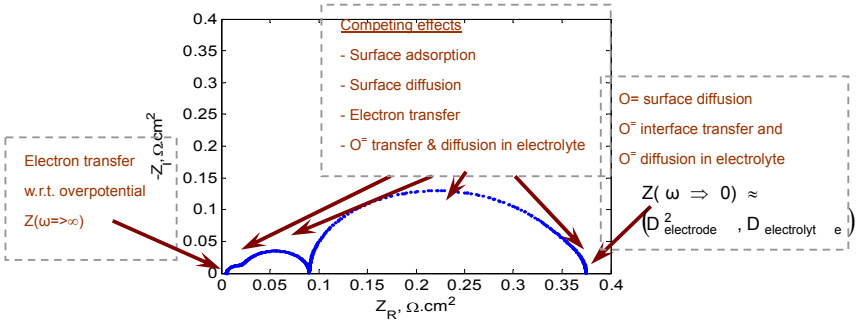

Figure 3: Governing physical mechanisms on EIS for oxygen reduction based on Model 2

tive parametric analysis of the simulated EIS for Model 2 and its comparison to experimental EIS measurements are presented in the following section. Here, we present the kinetics of the species and charge transport and their time and overpotential dependence described by Model 2 as:

$$\frac{d\theta_{ad,i}}{dt} = k_1 P_{O2} N_o (1-\theta_i)^2 - k_{-1} N_o \theta_i^2 - k_2 \theta_i + k_2 \alpha_i$$

$$\frac{d\alpha_i}{dt} = k_2 \theta_i - k_2 \alpha_i + \frac{D_i}{\Delta x^2}\left(\alpha_{i-1} - 2\alpha_i + \alpha_{i+1}\right) + \delta(i - n_{lsm})\left(-k_3 \alpha_i V_{\ddot{O}} + k_{-3} N_o O_{0_{YSZ}}\left(\theta_i - \alpha_i\right)\right)$$

$$\frac{dO_i}{dt} = \delta(i - 0_{YSZ})\left(k_3 \alpha_i V_{\ddot{O}} - k_{-3} N_o O_{0_{YSZ}}\left(\theta_i - \alpha_i\right)\right) + \frac{D_2}{\Delta x^2}\left(O_{i-1} - 2O_i + O_{i+1}\right)$$

where

$i = 1,2,...,n_{lsm-1},n_{lsm},0_{YSZ},0_{YSZ+1},...,m$

δ : Dirac Delta function

n_{lsm} : Section of LSM at 3PB; 0_{YSZ} : Section of YSZ at 3PB; m : Section in YSZ at its midpoint

θ : Surface coverage of adsorbed oxygen on LSM

α : Surface coverage fraction of reduced oxygen on LSM [5]

O : Normalized planaroxygen concentration in YSZ with respect to the surface of LSM

$\alpha_0 = 0, \alpha_{n_{lsm}+1} = 0,\ O_{m+1} = O_{m-1};\ k_2, k_{-2}, k_3, k_{-2}$ depend on the applied overpotetial

Definitions :

Adsorption activity : $A_A = k_1 P_{O2} N_o (1-\theta_i)^2$; Oxygen electronation activity : $A_E = k_2 \theta_i$

Oxygen transfer activity : $A_T = k_3 \alpha_i V_{\ddot{O}}$

Diffusion activity : $A_D = \frac{D_i}{\Delta x^2}\left(\alpha_{i-1} - 2\alpha_i + \alpha_{i+1}\right)$ and $A_Y = \frac{D_i}{\Delta x^2}\left(O_{i-1} - 2O_i + O_{i+1}\right)$

The predicted AC impedance spectroscopy signal response based on Model 2 is due to the total current from the electrode surface. The time-dependent concentrations of the intermediate species that contribute to the system current depend on the time constants of the complete model through the equations described in Eq. 5. Then, the current is:

$$I_F = -2FANo\left(k_2 \sum_{i,\,surface} \theta_i - k_2 \sum_{i,\,surface} \alpha_i\right) \quad [6]$$

Assumptions for Determining the LSM/YSZ Kinetic Parameters

The validity of the simulations from the modeling approach described in this paper depends on the material intrinsic kinetic properties such as the reaction rate constants, surface coverage of adsorbed oxygen, and diffusion coefficients, as well as the electrochemical model schemes. Some of the electrochemical data, such as the form of reactions and the reaction- and material-specific parameters can be found from the literature. However, available data are scarce for the LSM/YSZ system, compared to the possible details of realistic reaction schemes. Here, we summarize the literature information and assumptions that we used for the LSM/YSZ system:

1 – *The electrochemical models* retrieved from the literature and considered in this paper are presented in Table I. The ORR schemes for the surface of LSM described in Table I and others can take place individually or in parallel to each other. Here, we examine the models individually, in order to understand the physical implication of each on the AC impedance response.

2 – *The surface concentration of total oxygen sites, N_O,* affects how fast the oxygen gets adsorbed on or desorbed from the surface of LSM. We use the following range for N_O:

- $5x10^{-10} – 5x10^{-5}$ mols/m^2 (12,13)

3 – *Adsorption – desorption reaction rate constants, k_{ads}, k_{des}*, affect how fast the oxygen gets adsorbed on the surface of LSM. In finding these, we assume the following:

- The values of k_{ads} and k_{des} on LSM are close to that on a perovskite material. $3x10^{-5}$ mol.$cm^{-2}s^{-1}atm^{-1}$ and $2x10^{-8}$mol.$cm^{-2}s^{-1}$ for $Sm_{0.5}Sr_{0.5}CoO_3$ at 800 ^oC (14).
- The range of activation energy for surface adsorption-desorption is 150-250 kJ/mol.

4 – *Diffusion coefficients* for oxygen on the surface of LSM or for oxygen in YSZ influence how fast the charged species can be supplied to and removed from the LSM/YSZ interface. We use the following values for the oxygen diffusion coefficients:

- In the bulk of YSZ: $3.4x10^{-7}x \exp(-95530/RT)$ m^2/s (15)
- On the surface of LSM: 10^{-15} - 10^{-12} m^2/s (12,13)

5 – *Reduction/oxidation, and LSM/YSZ interface vacancy transfer rate constants* are not yet found in literature and are used parametrically in the current simulations.

ELECTROCHEMICAL KINETICS SIMULATIONS AND ANALYSIS

Simulations were performed to illustrate the features of EIS signals from ORR at LSM/YSZ described by Model 2. Important considerations in comparing the simulation results are: the change in the magnitude of Z and its components and the resonant frequency ranges as a function of the extrinsic and intrinsic properties of the system. The influence of the extrinsic and intrinsic properties of the LSM/YSZ system on the EIS from Model 2 can be categorized under three major motives: surface reactions, 3PB reactions, and bulk YSZ. Any change in operating conditions or material properties will affect either one or all of these motives. It is possible that not all the possible tendencies appear in the EIS measurements. This can be due to either the limited frequency range that can be captured by the impedance spectrometers or the relative dominance of particular motives over others in the impedance response. In order to evaluate the implications from AC impedance measurements, it is important to understand theoretically the tendencies in the EIS due to a change in any of the major motives. Therefore, we present a parametric analysis of EIS simulations where the individual effect of each process activity is reflected in the spectrum independently. In analyzing the simulated EIS, we consider two points to distinguish the governing process in a specific frequency range:

- If a resonant frequency shifts by changing a system property, then the specific process whose activity has been altered contributes to governing that frequency range.
- If a resonant frequency does not shift but the magnitude of the impedance in that frequency range changes, then the specific process whose activity has been altered does not contribute to governing that resonant frequency. However, the altered process changes the boundary conditions for another process(es) which governs the resonance.

Effect of Surface Reactions on the EIS of Model 2:

LSM surface reactions represented by Model 2 are controlled by adsorption and desorption of molecular oxygen, electronation (reduction) of oxygen, and diffusion of the reduced oxygen on the surface to the 3PB. A property change in the LSM/YSZ system can improve or degrade the activity of each of these reactions and influence the EIS respectively. Figures 4-6 represent the simulated effect of an increase in activity of each of these processes upon the EIS qualitatively based on Model 2 with $N_o=5x10^{-7}$mols/m^2. The improved activity represented in Figures 4-6 is an implication of an increase in the forward reaction rate constant or in the diffusion coefficient for the relevant process. Based on Model 2, the

activities of the molecular oxygen adsorption-desorption and adsorbed oxygen electronation reactions can predominantly govern the higher frequency region resonances, and influences only the magnitude of low frequency region impedance. In particular, the oxygen electronation step that corresponds to the current determines the high frequency intercept of impedance on the real axis, as shown analytically as well. The surface diffusion of the reduced oxygen shows its influence by shifting the resonant frequencies and the magnitude of impedance over both the high and medium frequency regions. Model 2 implies that the high frequency region can also be governed by electrode processes, contrary to findings in the literature (2,4,16) that assign the high frequency region solely to electrolyte processes.

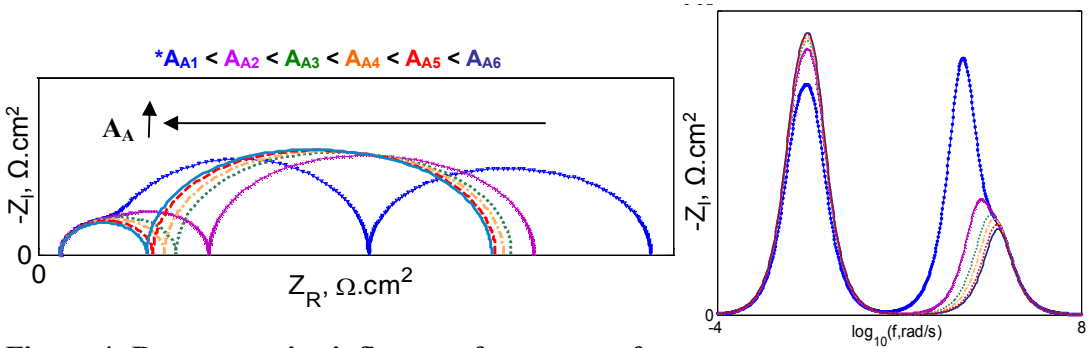

Figure 4: Representative influence of oxygen surface adsorption activity (A_A) on the AC impedance response predicted by Model 2 (*Variation on k_1:10^{11}-$5x10^{12}$ $((mols/m^2)s.atm)^{-1}$

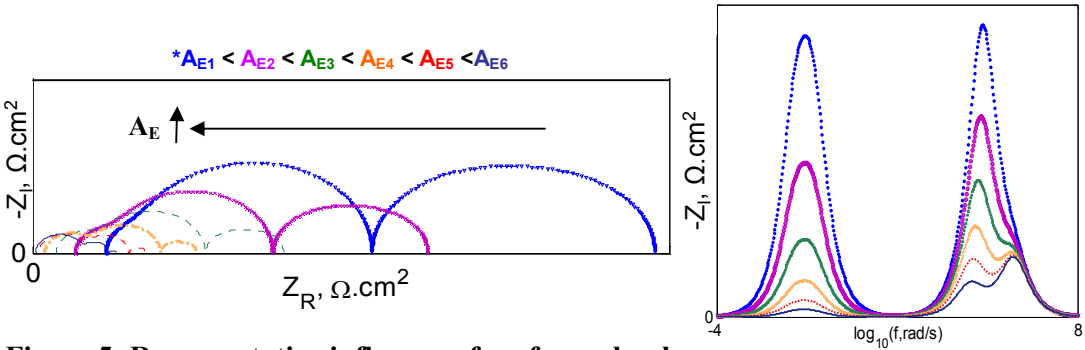

Figure 5: Representative influence of surface-adsorbed oxygen electronation activity (A_E) on the AC impedance response predicted by Model 2 (*Variation on k_2: 10^6-$3x10^7$ s^{-1})

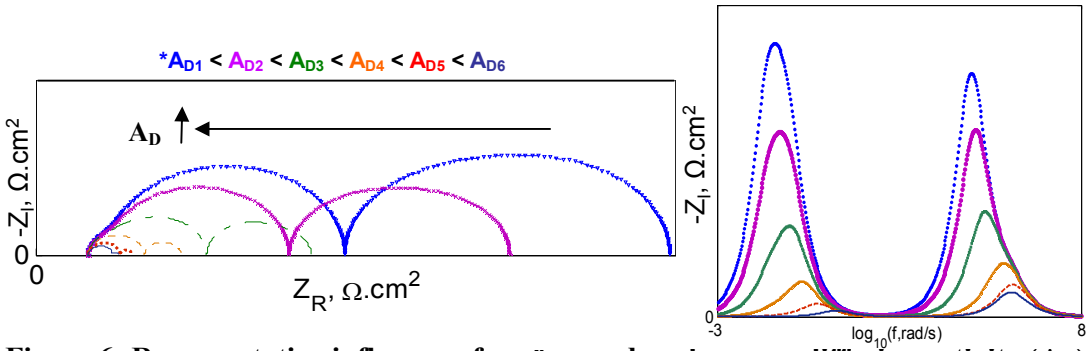

Figure 6: Representative influence of surface-reduced oxygen diffusion activity (A_D) on the AC impedance response predicted by Model 2 (*Variation on $D_{surface}$: 10^{-15}-10^{-12} m^2/s)

Effect of 3PB Reactions on the EIS of Model 2:

3PB reactions of LSM/O_2/YSZ represented by Model 2 are controlled by reactions same as on LSM surface in addition to $O^{=}$ transfer between LSM and YSZ. Figure 7 represents the simulated effect of the improvement in activity of $O^{=}$ transfer at the interface upon the EIS

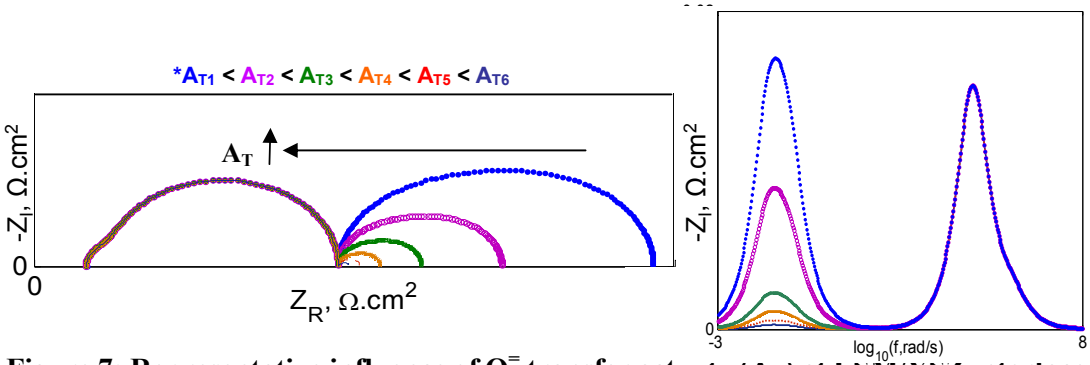

Figure 7: Representative influence of $O^{=}$ transfer activity (A_T) at LSM/YSZ interface (3PB) on the AC impedance response from Model 2 (*Variation on k_3: 10^6-10^8 $((mols/m^3)s)^{-1}$)

qualitatively based on Model 2 with N_o=5x10^{-7}mols/m^2. The improved activity simulated for Figure 7 is an implication of an increase in the forward reaction rate constant. It is shown in Figure 7 that the $O^{=}$ transfer activity at LSM/YSZ interface can influence the magnitude of the low frequency in EIS, but does not contribute to the resonant frequency in that region.

Effect of YSZ on the EIS of Model 2:

The contribution of the YSZ electrolyte to the O_2 reduction process in Model 2 is represented by the removal of oxygen from the 3PB with diffusion along the oxygen concentration gradient within the bulk of the electrolyte. Figure 8 represents the simulated effect of an increase in activity of oxygen diffusion in YSZ upon the EIS qualitatively based on Model 2 with N_o=5x10^{-7}mols/m^2. The oxygen diffusion in the YSZ electrolyte as described by Model 2 governs the low frequency region of the EIS, by both shifting the resonant frequency and by varying the magnitude of impedance. In certain configurations of kinetic properties, it can shift towards the high frequency region and interfere with the other peaks. However, it is most extensive at the low frequencies. The dominance of diffusion at low frequencies is noted in Ref.1,p.105. Some literature attributed the high frequency response to oxygen diffusion in YSZ (2,4,16). Oxygen reduction in LSM/YSZ based on Model 2 does not confirm this assumption. As also shown in Figure 3, Model 2 including the YSZ oxygen diffusion indicates that the low frequency response and the low frequency intercept at the real axis are governed significantly by oxygen diffusion in the electrolyte.

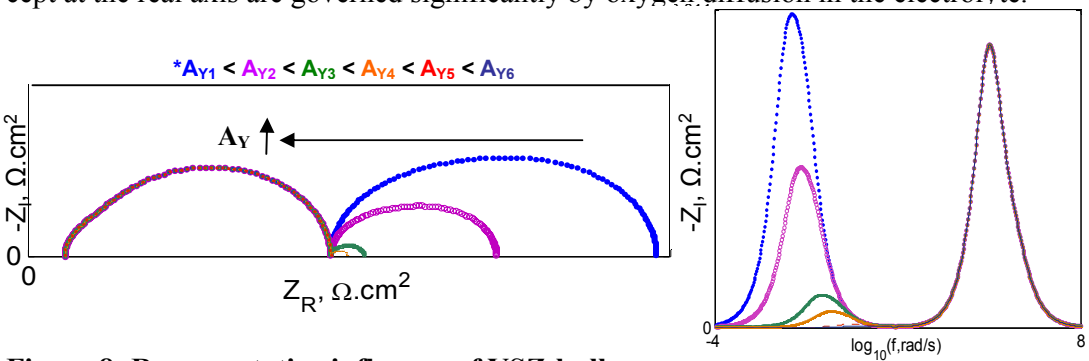

Figure 8: Representative influence of YSZ-bulk oxygen diffusion activity (A_Y) on the AC impedance response from Model 2 (*Variation on D_{YSZ}: 10^{-12}-10^{-10} m^2/s)

Comparison of Model 2 EIS Simulations to Experimental EIS:

As P_{O2} is altered, it can influence the surface reactions in a coupled manner and can yield a variation in the EIS as a combination of those presented in Figures 4-6 individually. Figure

9-a and 9-b represent the measured EIS (as discussed in Part I of this paper) and the simulated EIS for 1 atm of P_{O2} at 800°C. Figure 9-b is the result of simulation of Model 2 EIS based on the assumptions listed in the previous section and is the one that can get closest to the measured EIS within the range of those assumptions. As P_{O2} is altered to lower values, the experimental EIS indicates that the lower frequency arc becomes wider with less curvature while negligibly small change is observed for the high frequency arc, as shown in Figure10-a. However, the simulated EIS based on Model 2, which could closely reproduce the experimental EIS for P_{O2}=1atm at 800°C, indicates significant changes over the complete frequency range, as shown in Figure 10-b. This implies that Model 2 which can be likely to describe oxygen reduction on LSM is not exactly the governing reaction mechanism for the LSM microelectrodes in our work. The discrepancy between the experimental and the simulated EIS can be either due to a mismatch between the actual reaction steps or due to a change in some intrinsic parameters as a function of P_{O2} that is not accounted for in this model as of yet.

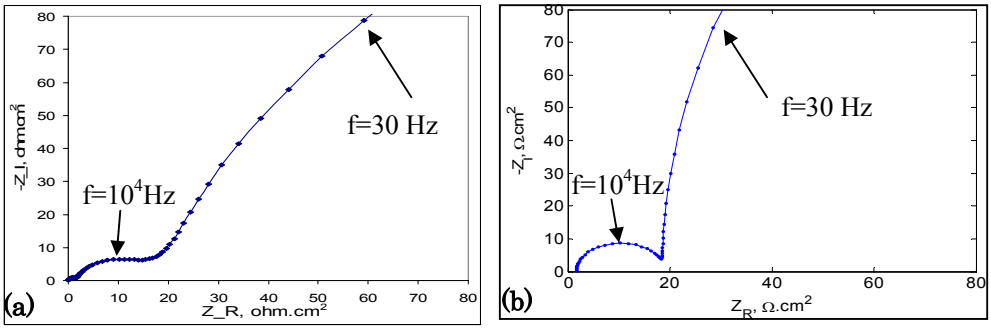

Figure 9: (a) Experimental and (b) simulated EIS for LSM microelectrode at 800°C and P_{O2} value of 1atm

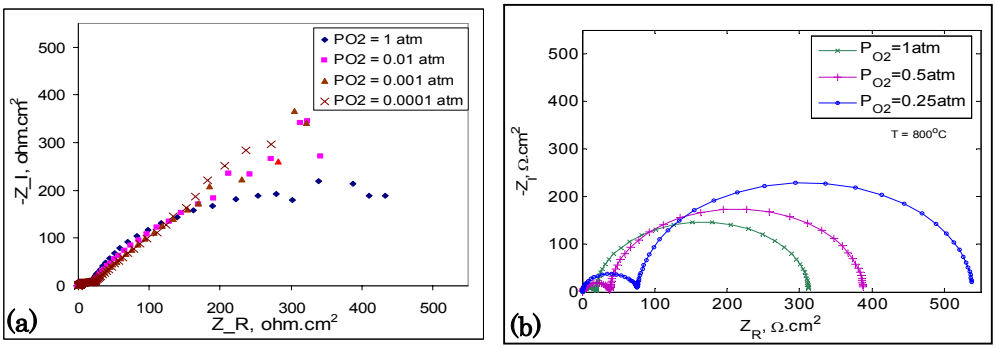

Figure 10: (a) Experimental and (b) simulated EIS for LSM microelectrode as a function of P_{O2} at 800°C.

CONCLUSIONS AND FUTURE WORK

The electrochemical modeling and simulations carried out in this work can effectively describe the AC impedance response directly from a detailed electrochemical model at the molecular level. The analytical and simulated EIS allows us to gain an insight of the influence of each property of the system on its AC impedance response. The coupling of the AC impedance experiments with patterned microelectrodes can verify the primary reaction mechanisms and the kinetic model parameters. Therefore, an extensive amount of experiments are necessary to confirm the uniqueness of the proposed detailed oxygen reduction models and the accompanying kinetic parameters. The number of experimen-

tally varied parameters must match or be close to the number of unknown parameters in the electrochemical models in order to confirm the validity of the proposed electrochemical mechanism. The experimental approach of our work with this purpose is presented in Part I of this paper. The Model 2 that is based on indications from literature and simulated so far extensively in this paper cannot describe the P_{O2} dependence of EIS experiments on LSM microelectrodes of this study. A comparison of the simulated and experimental EIS as a function of P_{O2} indicates discrepancy between the two. Thus, the ORR model requires modifications. Further detailed studies are required, both experimentally and analytically, before the electrochemical models for oxygen reduction at LSM/YSZ can be confirmed in our work. For the model development progress, two-step electron transfer, diffusion of atomic adsorbed oxygen on LSM, bulk diffusion of reduced oxygen in LSM and electrochemically active electrolyte possibilities should be considered.

ACKNOWLEDGMENTS

This work was financially supported by the U.S. Department of Energy, Office of Technology Support Programs, under Contract Number W-31-109-ENG-38 at Argonne National Laboratory and by the FORD-MIT Alliance. This work made use of the Shared Experimental Facilities supported by the MRSEC Program of the National Science Foundation under award number DMR 02-13282. We would also like to thank Dr. Mark Petri for carefully proofreading this manuscript.

REFERENCES

1. J. R. Macdonald, *Impedance Spectroscopy: Emphasizing solid materials and systems,* John Wiley & Sons, (1987).
2. S. P. Jiang, *Solid State Ionics,* **146**, 1 (2002).
3. S. P. Jiang, J. G. Love, Y. Ramprakash, *Journal of Power Sources,* **110**, 201 (2002).
4. E. P. Murray, T. Tsai, S. A. Barnett, *Solid State Ionics,* **110**, 235 (1998).
5. T. Ioroi, T. Hara, Y. Uchimoto, Z. Ogumi, Z. Takehara, *Journal of the Electrochemical Society,* **144**, 1362 (1997).
6. X. J. Chen, K. A. Khor, S. H. Chan, *Journal of Power Sources,* **123**, 17 (2003).
7. M. J. Jorgensen, M. Mogensen, *Journal of the Electrochemical Society,* **148**, A433 (2001).
8. A. Bieberle, L. J. Gauckler, *Solid State Ionics* **146**, 23 (2002).
9. A. Mitterdorfer, L. J. Gauckler, *Solid State Ionics* **117**, 203 (1999).
10. A. Mitterdorfer, L. J. Gauckler, *Solid State Ionics* **117**, 187 (1999).
11. M. Prestat, L. J. Gauckler, in *4th European SOFC Forum Proceedings,* p.679 (2000).
12. H. Ullmann, N. Trofimenko, F. Tietz, D. Stover, A. Ahmad-Khanlou, *Solid State Ionics,* **138**, 79 (2000).
13. H. Fukunaga, M. Ihara, K. Sakaki, K. Yamada, *Solid State Ionics,* **86-8**, 1179 (1996).
14. H. Fukunaga, M. Koyama, N. Takahashi, C. Wen, K. Yamada, *Solid State Ionics,* **132**, 279 (2000).
15. M. Kilo, C. Argirusis, G. Borchardt, R., Jackson, *Phys. Chem. Chem. Phys.*, **5**, 2219 (2003)
16. J. D. Kim, G. D. Kim et al., *Solid State Ionics,* **143**, 379 (2001).